Computational Mechanics
Research and Support
for Aerodynamics and Hydraulics
at **TFHRC**

Argonne
NATIONAL LABORATORY
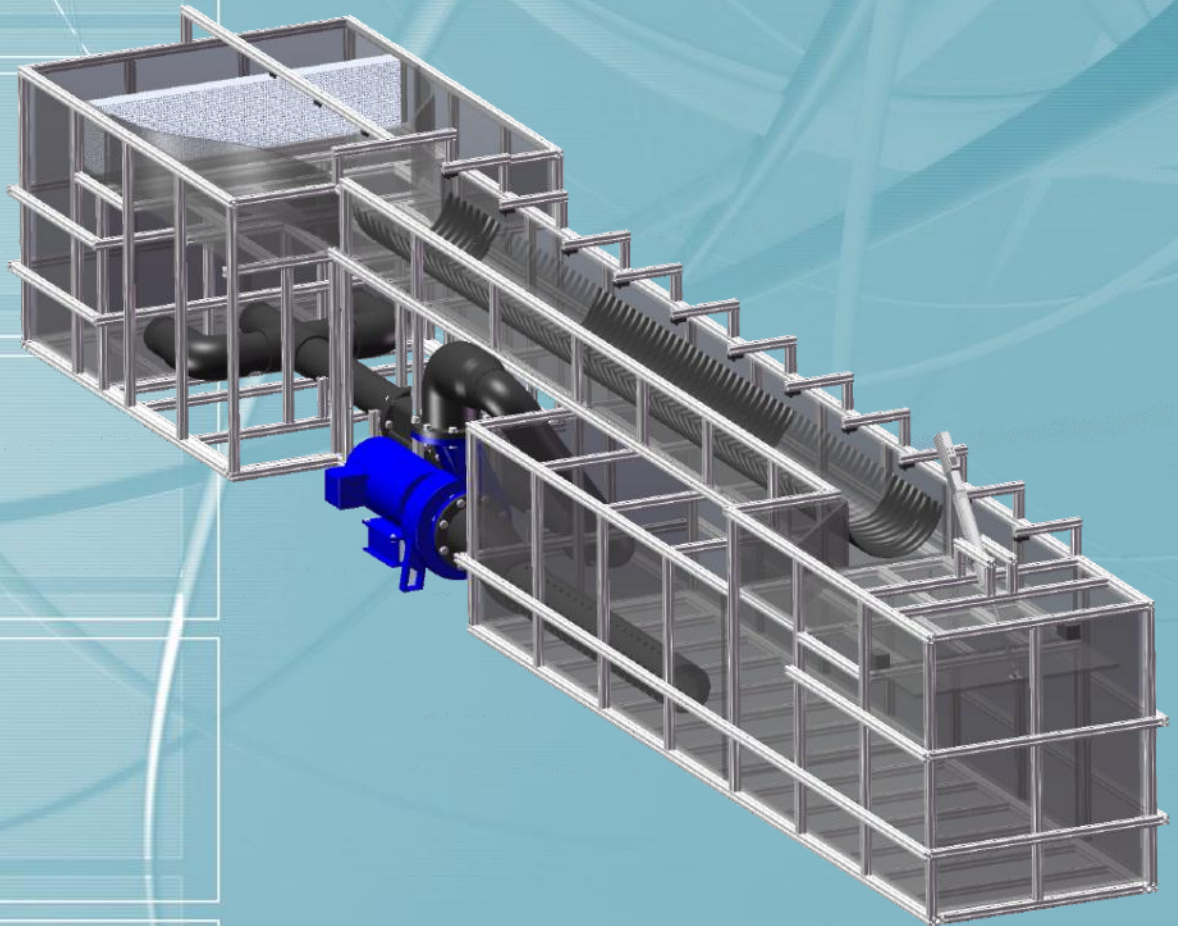
Culvert Analysis Quarterly Report

April through June 2011

Computational Fluid Dynamics Modeling of Flow through Culverts
2011 Quarter 3 Progress Report

Energy Systems Division (ES)
Argonne National Laboratory (ANL)

Principal Investigator:
Steven A. Lottes, Ph.D.

Contributing CFD Investigators:

Sudhir Lanka Venkata
Pradip Majumdar, Ph.D.
Northern Illinois University

Yuan Zhai
University of Nebraska

July, 2011

Table of Contents

List of Figures

List of Tables

1.   Introduction and Objectives

This project was established with a new interagency agreement between the Department of Energy and the Department of Transportation to provide collaborative research, development, and benchmarking of advanced three-dimensional computational mechanics analysis methods to the aerodynamics and hydraulics laboratories at the Turner-Fairbank Highway Research Center (TFHRC) for a period of five years, beginning in October 2010. The analysis methods employ well-benchmarked and supported commercial computational mechanics software and also include user subroutines, functions, and external software programs and scripts written to automate the analysis procedures. Computational mechanics encompasses the areas of Computational Fluid Dynamics (CFD), Computational Wind Engineering (CWE), Computational Structural Mechanics (CSM), and Computational Multiphysics Mechanics (CMM) applied in Fluid-Structure Interaction (FSI) problems.

This quarterly report documents technical progress on the CFD modeling and analysis of flow through culverts for the period of April through June 2011. The focus of effort for the work this year is on improving methods to assess culvert flows for fish passage.

2.   Computational Modeling and Analysis of Flow through Large Culverts for Fish Passage

Fish passage through culverts is an important component of road and stream crossing design. As water runoff volume increases, the flow often actively degrades waterways at culverts and may interrupt natural fish migration. Culverts are fixed structures that do not change with changing streams and may instead become barriers to fish movement. The most common physical characteristics that create barriers to fish passage include excessive water velocity, insufficient water depth, large outlet drop heights, turbulence within the culvert, and accumulation of sediment and debris. Major hydraulic criteria influencing fish passage are: flow rates during fish migration periods, fish species, roughness, and the length and slope of the culvert.

The objective of this work is to develop approaches to CFD modeling of culvert flows and to use the models to perform analysis to assess flow regions for fish passage under a variety of flow conditions. The flow conditions to be tested with CFD analysis are defined in the tables of a work plan from TFHRC [6]. The CFD models are being verified by comparing computational results with data from experiments

conducted at TFHRC. A primary goal of CFD analysis of culverts for fish passage is to determine the local cross section velocities and flow distributions in corrugated culverts under varying flow conditions. In order to evaluate the ability of fish to traverse corrugated culverts, the local average velocity in vertical strips from the region adjacent to the culvert wall out to the centerline under low flow conditions will be determined.

A primary goal of the CFD analysis during this quarter has been to determine the local velocities and flow distributions through culverts for the fish passage with no gravel in the culvert. In order to more accurately evaluate the ability of fish to traverse culverts, it is desirable to look at the changes in the local average velocity of the flow adjacent to the culvert wall under low flow conditions. CFD runs using the cyclic boundary conditions to obtain the fully developed flow on a reduced 3D section of the culvert (symmetric quarter of the culvert section with corrugations from trough to another trough) have been conducted using CD-adapco's STAR-CCM+ software. Use of the cyclic boundary condition requires an assumption of a nearly flat water surface that can be modeled with a symmetric boundary condition that allows a free slip water velocity at that boundary. The cyclic boundary approach shortens the simulation time required to establish a fully developed flow with a known mass flow rate (with this approach several test cases can be completed per day). The periodic fully developed condition is achieved by creating a cyclic boundary condition, where all outlet variables are mapped back to the inlet interface, except for the pressure because there is a pressure drop corresponding to the energy losses in the culvert section. The pressure jump needed to balance the pressure drop for the specified mass flow is iteratively computed by the CFD solver. The runs were conducted with various mesh sizes, to take a closer look at how the velocity distribution and other flow parameters vary at different locations of the flow field by varying the base size of the mesh to obtain solutions that are effectively mesh independent. The mesh refinement study is also used to identify meshes that are computationally efficient while yielding good mesh independent results. An investigation of how the flow field varies for different cases such as reduced culvert section when considered from a trough to trough versus crest to crest. The computational model is based on the three-dimensional transient RANS k-epsilon turbulence model with wall function treatment.

The modeling work was done in collaboration with staff at TFHRC conducting physical experiments of culvert flows for the fish passage project in the Federal Highway Administration (FHWA). A preliminary comparison of the velocity distribution on the trough section between CFD model results and laboratory observation data was conducted. The 3D CFD model solves the Reynolds averaged Navier-Stokes (RANS) equations with k-epsilon turbulence model with wall function. The VOF method, which captures the free surface profile through use of the variable known as the volume of fluid was used in the multi-phase CFD model. The verification of the CFD model for engineering application using the laboratory observation data is a key step for the further work. A comparison of the multi-phase model and full scale flume single phase model was also done.

2.1. Model of Culvert Section with Fully Developed Flow Using Cyclic Boundary Conditions

In this study, a simulation model was developed using the commercial CFD software STAR-CCM+. A small section of the culvert barrel was modeled with cyclic boundaries at the inlet and outlet sections of the computational domain. A 36 inch diameter culvert with corrugation size 3 inches by 1 inch has been used for this study. The flow depth was 9 inches, a flow velocity was 0.71 feet/second, and zero bed elevation in the culvert (no gravel present).
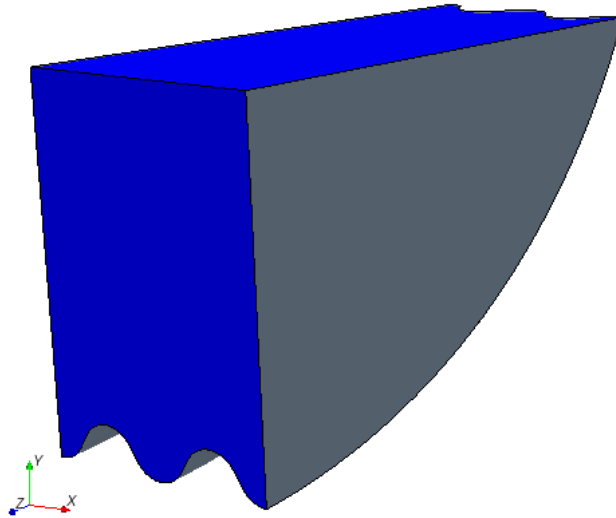
Figure 2.1: Reduced symmetric section of the barrel considered from a trough to trough

The boundary conditions used for the computational model in Figure 2.1 are listed in Table 2.1 below. All the CFD runs have been carried out with the same set of boundary conditions.

Table 2.1: Boundary conditions

Boundary	Name	Type
Face at minimum x value	Inlet	Cyclic boundary condition
Face at maximum x value	Outlet	Cyclic boundary condition
Water surface	Top	Symmetry plane
Centerline	Center	Symmetry plane
all other surfaces	Barrel	No-slip wall

2.2.   Mesh Refinement Study

As detailed in the previous quarterly report, a CFD procedure is being developed to test the flow conditions that are defined in the tables of the work plan from TFHRC [6]. As a part of developing the procedure, mesh refinement studies are being conducted for each geometry configuration in the work plan. Sensitivity to mesh refinement will need to be checked for the larger culverts in the work plan when the geometry for those culverts are built. In the process of mesh refinement various base sizes have been chosen, along with the creation of a volumetric control (annulus ring) along the corrugated section. The refinement of the mesh is defined by specifying a reduction of mesh size for volume within an annulus intersecting the model as shown in Figure 2.2. The volumetric control body intersecting the corrugated section provides a means to refine the mesh in the corrugated region of interest. The refined mesh enables better resolution of the flow field with recirculation zones at the troughs between the corrugations. Meshing also includes a prism layer consisting of orthogonal prismatic cells running parallel to the wall boundaries, which constitutes a boundary mesh that is good for the application of wall functions to compute the shear stress at the wall boundaries.
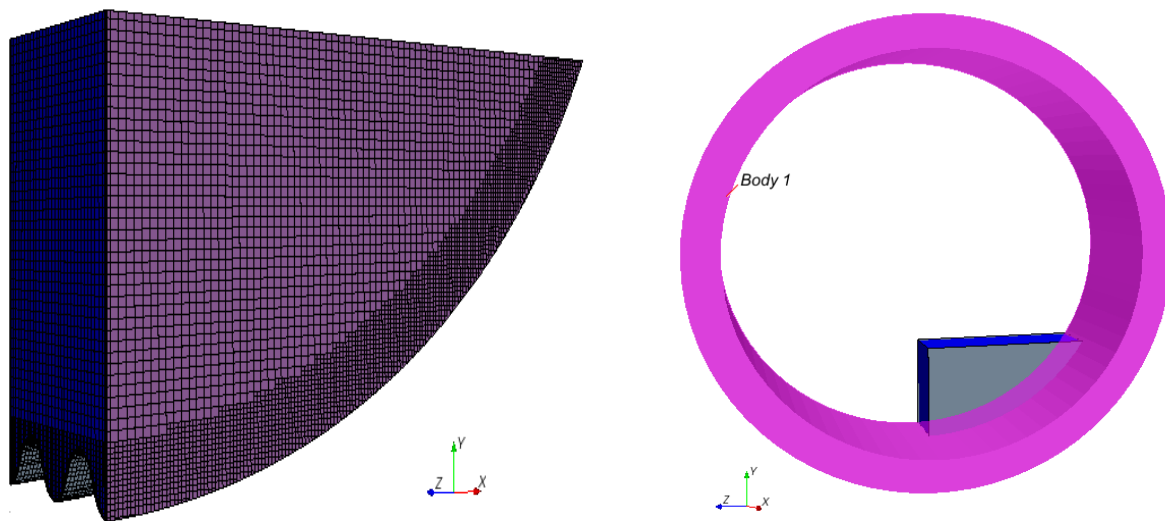
Figure 2.2: Refined mesh area with respect to the base created using a volumetric control

A volumetric control (annulus ring) was created intersecting the corrugated section to specially refine the mesh around this region with respect to the base as shown in Figure 2.2. Figure 2.3 does not show a coarser version of mesh 1 and mesh 4 because they look similar to mesh scenes 2 and 5 with larger cells. Sensitivity of the solution was tested with 6 variations of the mesh, including two base sizes and 4 combinations of refinement in the region with the corrugations where recirculation zones develop. The refinement is defined by specifying a reduction of mesh size for volume within a volumetric control as shown in Figure 2.2.
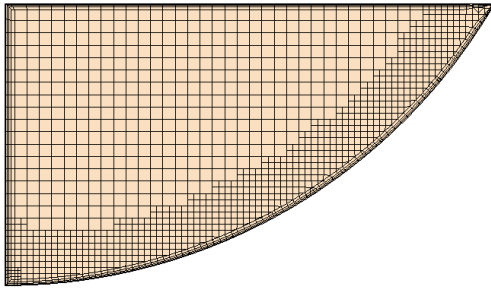
Mesh 2 Base 10 mm, 50% Wall Zone Refinement
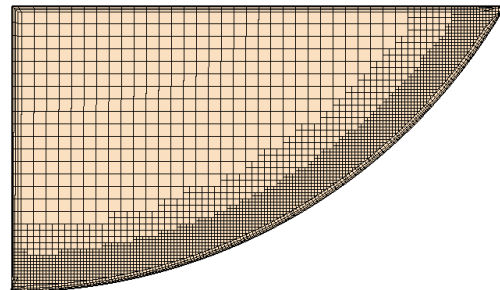
Mesh 3 Base 10 mm, 30% Wall Zone Refinement
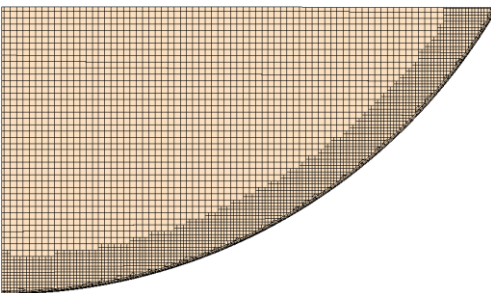
Mesh 5 Base 5 mm, 67% Wall Zone Refinement
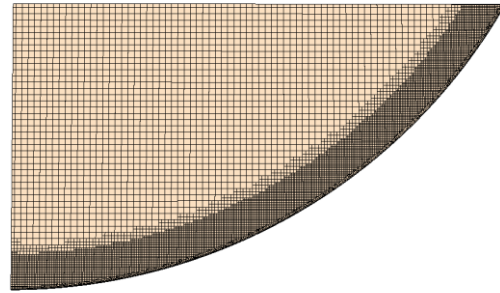
Mesh 6 Base 5 mm, 40% Wall Zone Refinement

Figure 2.3: Mesh scenes of the various cases used for mesh refinement studies

Table 2.2 below summarizes the details of the different cases considered in the mesh refinement study. For meshes 1 and 4, a uniform mesh size distribution with a mesh size of 10 mm and 5mm respectively has been chosen, other mesh types in Table 2.2 use volume controls for meshing to achieve a finer mesh with increased number of cells near the corrugated wall region to better resolve the recirculation zones in the region. A specified mass flow rate is given at the inlet and the outlet, which are the cyclic boundaries to obtain the cyclic fully developed flow condition. A mass flow rate of 13.85 kg/s was set for the cyclic boundary condition. The mass residuals decrease slightly for finer meshes, are good for all meshes, and don't nessarily indicate the accuracy of the computation.. The accuracy of the results obtained in terms of the velocity profiles at different sections in the flow field or the visualized scenes give a better picture of sensitivity to the mesh. The degree of convergence does not indicate the amount of discretion error. When the flow is not parallel to the cells in the mesh, there is some difference in the mass flow obtained by integrating over the cyclic boundary interface and a plane midway through the culvert section which gives some discretion error. The corrugations cause the flow streamlines to curve and not remain parallel to the mesh. Column 5 from Table 2.2 indicates the percent deviation of the mass flow across the boundary and mid plane. These values are all very good except for the coarsest mesh.

Table 2.2: Details of the various meshes used in the mesh refinement study

| Case	Base size (m)	%Refinement in Corrugation Zone	Cells in Mesh	Mass Residual	% Deviation in Cross Section Mass Flow at a trough(mid-plane)	% Deviation in Cross Section Mass Flow at a crest
Mesh 1	0.01	None	18,910	2.32×10^{-7}	0.010	0.1
Mesh 2	0.01	50	58,803	2.44×10^{-7}	-0.005	0.002
Mesh 3	0.01	30	202,168	1.97×10^{-7}	0.008	0.018
Mesh 4	0.005	none	108,978	1.24×10^{-8}	0.029	-0.010
Mesh 5	0.005	66.6	249,174	3.35×10^{-8}	0.009	0.005
Mesh 6	0.005	40	887,369	2.8×10^{-8}	0.016	0.015
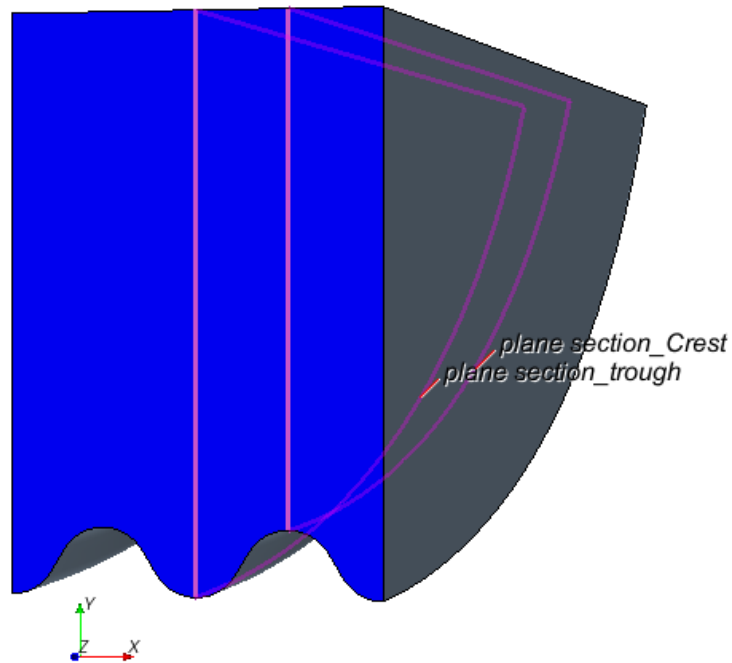
Figure 2.4: Sectional planes created at the trough and the crest to resolve flow parameters

Figure 2.4 shows the outline of plane sections defined in the geometry at a crest and a trough for analyzing the flow field velocity variation over culvert cross sections. The velocity distribution is analyzed by creating thin uniform strips, these uniform thin strips were created on a plane section (at the second trough in this particular case) using the post-processing features available in the STAR-CCM+ software.
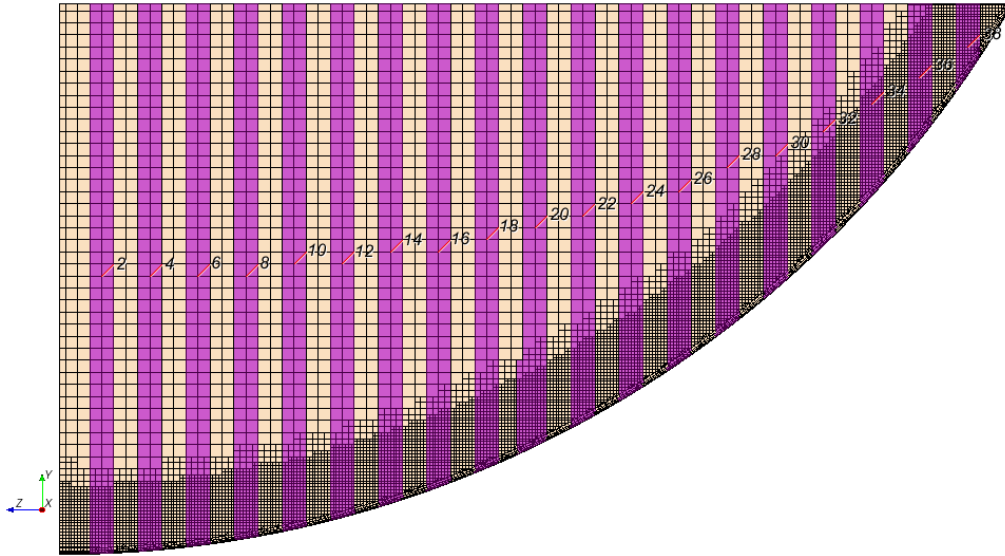

Figure 2.5: Uniform strips created using "Thresholds" feature available in STAR-CCM+

The uniform strips were created on the plane section at a trough in this case. Figure 2.5 shows only the even numbered strips created on the plane section at a trough. This procedure is carried out by creating multiple "Thresholds" of 1 cm width along the plane section. They are aligned with cell faces to avoid some interpolation error and obtain the best mean strip averaged velocity based on cell centroid values. After the thresholds are created, there is a "Report" feature available in STAR-CCM+ which calculates the surface averaged velocity of the uniform strip object.

2.2.1. Simulation Results and Discussion

2.2.1.1. Variation of the Surface-averaged Velocity over the Length of the Cross Section Studies:

In Figure 2.6 the trends of the curves (surface-averaged velocities on the plane section at the second trough) are plotted in MS-Excel along the length of the section. The x axis of the plot indicates the length of the plane section and the y-axis of the plot indicates the surface-averaged velocity. Each of these cases have the same base size of 10mm and refinement in the corrugated section for the two cases differ as mentioned in the plot are shown. For mesh 1, the curve indicating the trend of the surface-averaged velocity is irregular. Further, as the mesh is refined in the corrugated section the curves

indicating the surface averaged velocity of each of the uniform strips along the length of the plane section smooth out indicating that mesh refinement definitely affects the nature of the curve.
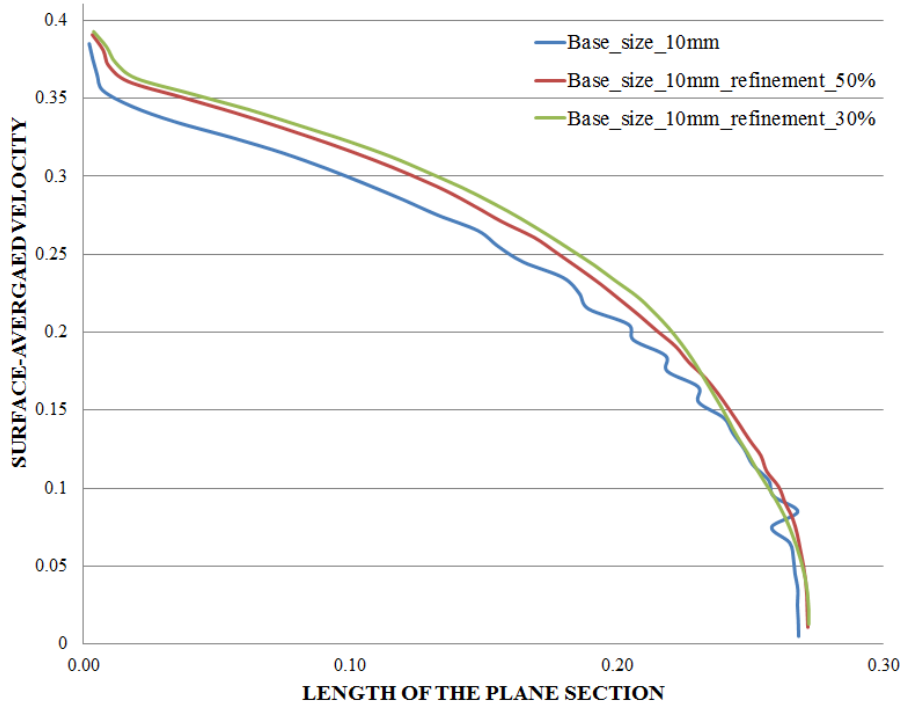

Figure 2.6: Surface averaged velocity vs. length of the plane section (created at a trough) plot for meshes 1-3

While looking at the curve for mesh 3, it is observed that the surface-averaged velocity along the uniform strips is not smoothened and the pattern of the curve is still indefinite with irregularities. This behavior of the curve for mesh 3 suggests that the flow resolution of the CFD model is grid independent beyond a particular value of mesh refinement. Thus the procedure of creating "Thresholds" and generating reports to output the surface-averaged velocity for various mesh cases helps in identifying the optimum value of the base size of the mesh and also the extent to which the mesh could be refined in the corrugated section.

The same procedure of creating the strips using thresholds and generating the reports is followed for meshes 4-6, the only difference here being the base size of the mesh is 5 mm. A volumetric control is used in the corrugated section for mesh 5 and 6 where the mesh is further refined in comparison with the base size of the mesh. The curve for mesh 4 is observed to be smooth. When the mesh 5 is further refined, the surface-averaged velocity plotted along the length of the cross section is slightly different

from that of mesh 4 but close, and either would be adequate for engineering purposes. When the corrugated section is further refined with respect to the base in case of mesh 6, the path of the curve is initially as expected but contains an irregular ripple. The cause of this effect is currently unknown.
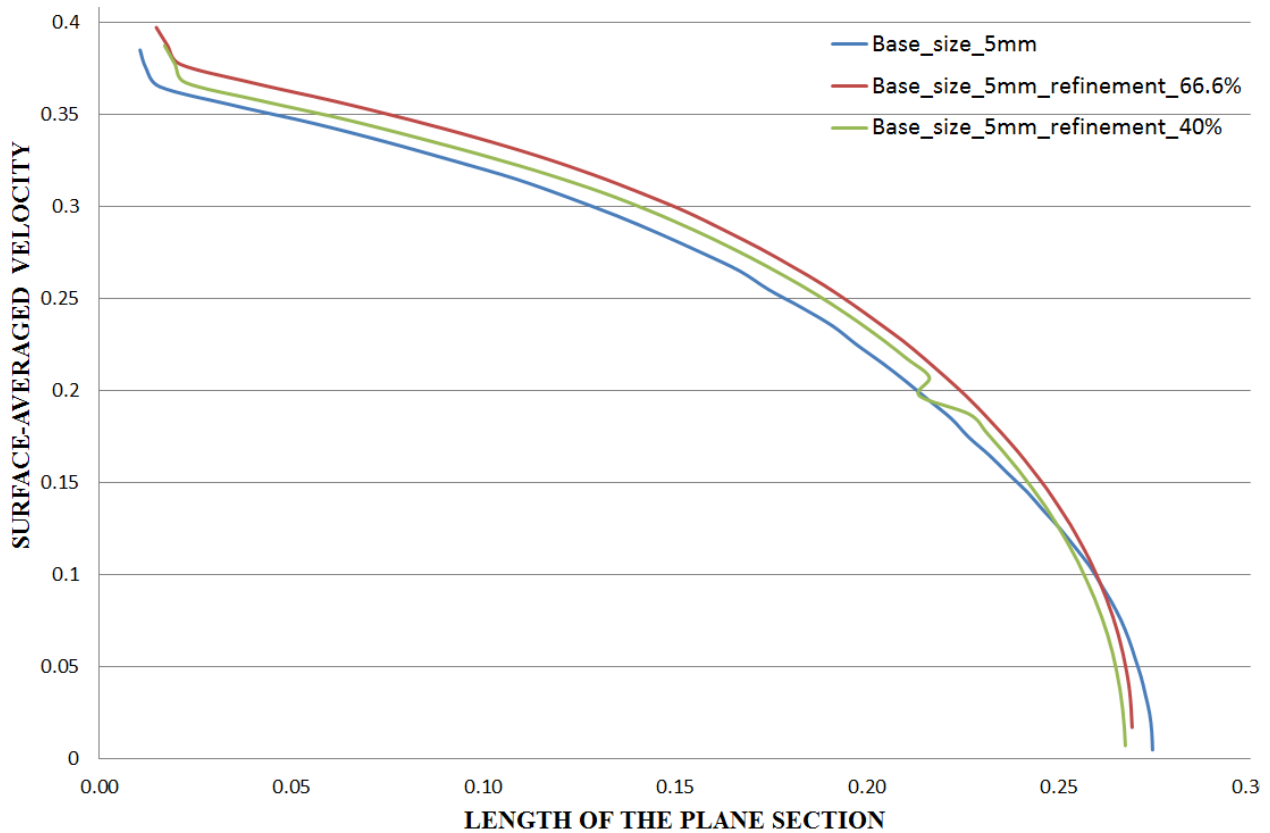
Figure 2.7: Surface averaged velocity vs. length of the plane section (created at a trough) plot for meshes 4-6

2.2.1.2. Velocity Profile Variation with Mesh Refinement

Line probes have been created along the flow section in the STAR-CCM+ software. In this particular case line probes have been created at a trough and a crest which are the regions of major interest. Each of the line probes created has 30 points on the line. The value of the Velocity magnitude of the flow is extracted at that particular point. Velocity profiles have been plotted using the line probes at a trough and a crest along the reduced barrel section. By taking a close look at the velocity profiles, it is possible to better analyze the nature of the flow.
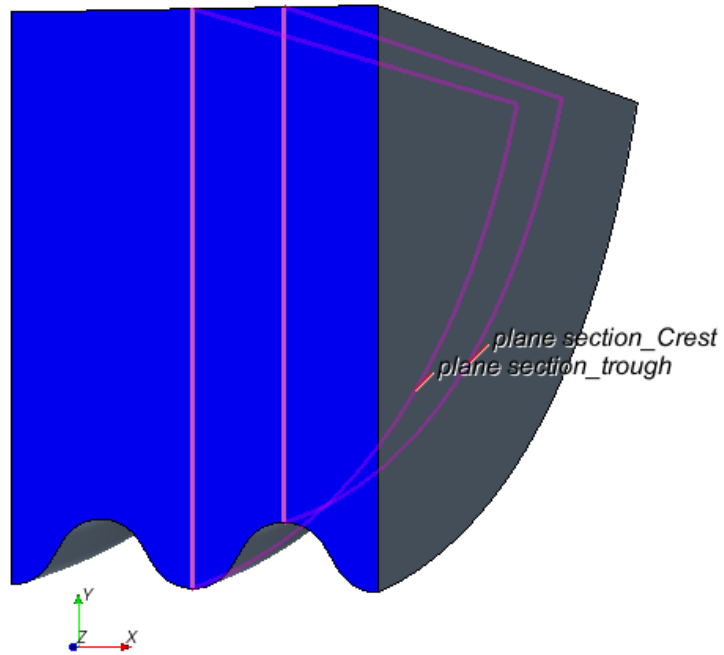
Figure 2.8: Line probes created at a trough and a crest along the flow field in the reduced barrel
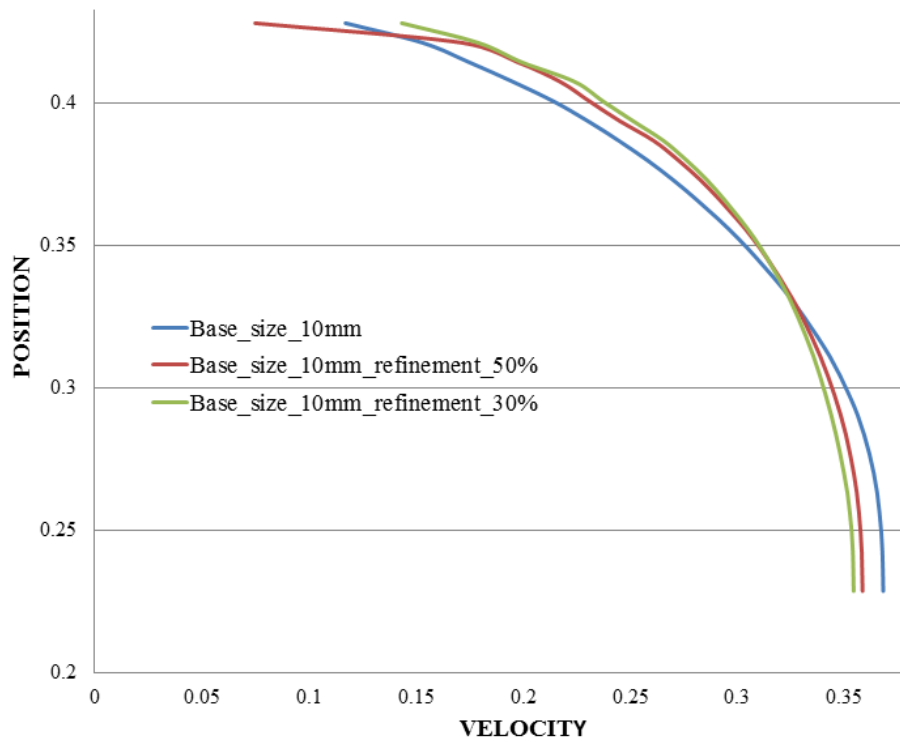

Figure 2.9: Velocity profiles of the different mesh cases with base size as 10mm plotted at a crest

In Figure 2.9, the x –axis of the plot represents velocity and the y-axis represents the position of the line probe at a trough in the vertical direction. The minimum unit on the y-axis is 0.2 m and the maximum unit is 0.4572 m. The y coordinate of the boundary representing the water surface (namely the top of the reduced culvert section in the CFD study) is at 0.2286 m and the y coordinate of the boundary representing the bottom of the culvert at the wall in 0.4572 m. The same CAD model has been used for all the CFD simulations with the co-ordinates of the reduced symmetric barrel section considered from a trough to a trough as mentioned above. The top surface of the culvert is simulated as a symmetry plane as mentioned previously which represents an imaginary plane of symmetry in the simulation. It implicates an infinitely spread region modeled as if in its entirety. The bottom of the culvert is simulated as a wall with a no slip condition. When velocity is plotted against position, the velocity at the wall is zero, the first point plotted is the velocity in the cell next to the wall and increases with distance from the wall. In Figure 2.9, the velocity profiles change as the base size of the mesh is varied. All of these cases show some mesh dependence but may be adequate for engineering analysis of fish passage. However, because cases using the relatively small geometry of a barrel section with periodic boundary conditions complete in a short time further mesh refinement was investigated.
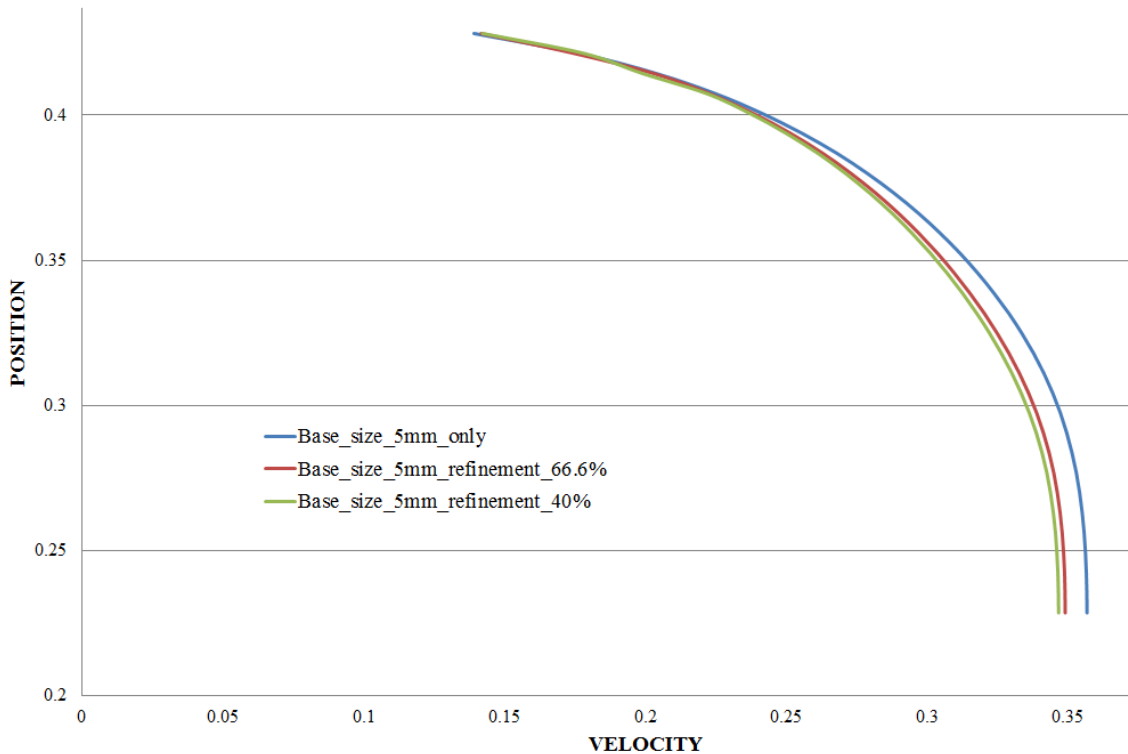

Figure 2.10: Velocity profiles of the different mesh cases with base size 5mm plotted at a crest

In Figure 2.10 the velocity and the position corresponding to the line probe (at a crest) are represented on the x and y axis of the plot. With a mesh base size of 5mm, the velocity profiles are very regular. For the mesh case where the base size is 5mm and no refinement in the corrugated section, the maximum velocity is a little higher than cases with further refinement in the corrugations. For mesh cases 5 and 6 where the mesh is further refined along the corrugated section in the order of 80% and 66% respectively there is not much difference in the nature of the velocity profiles although there is large difference in the number of computational cells. Mesh case 5 consists of 249,174 cells and mesh case 6 consists of 887,369 cells. Mesh 5 is reasonably mesh independent upon further refinement and consumes a reasonably small amount of computational resources.
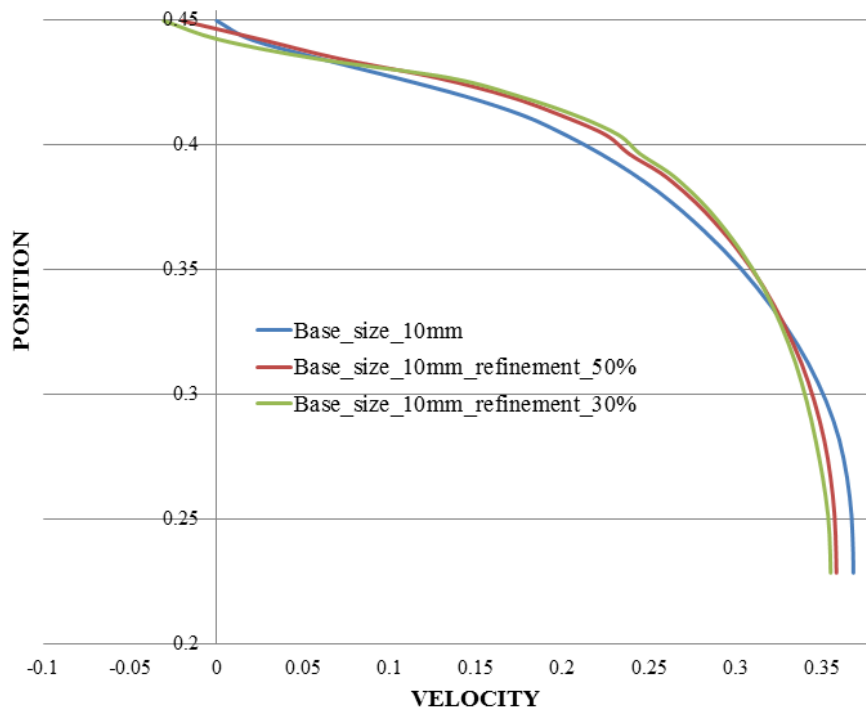

Figure 2.11: Velocity profiles of the different mesh cases with base size 10mm plotted at a trough

In Figure 2.11 the velocity profiles of the various mesh cases with base size 10 mm are plotted at a trough using line probes. The x-axis has a negative scale due to reverse flow in the recirculation zones in a trough. One of the benefits of flow simulation is that it provides detailed information about recirculation. Recirculation regions in the flow field are of particular interest since their presence can have a significant impact on the nature of the flow. As seen in Figure 2.11, there is a difference in the velocity profiles for the various mesh cases. The mesh case 4 has not been able to capture the effect of flow recirculation, but as the mesh is further refined along the corrugated section the recirculation of the flow can be resolved.
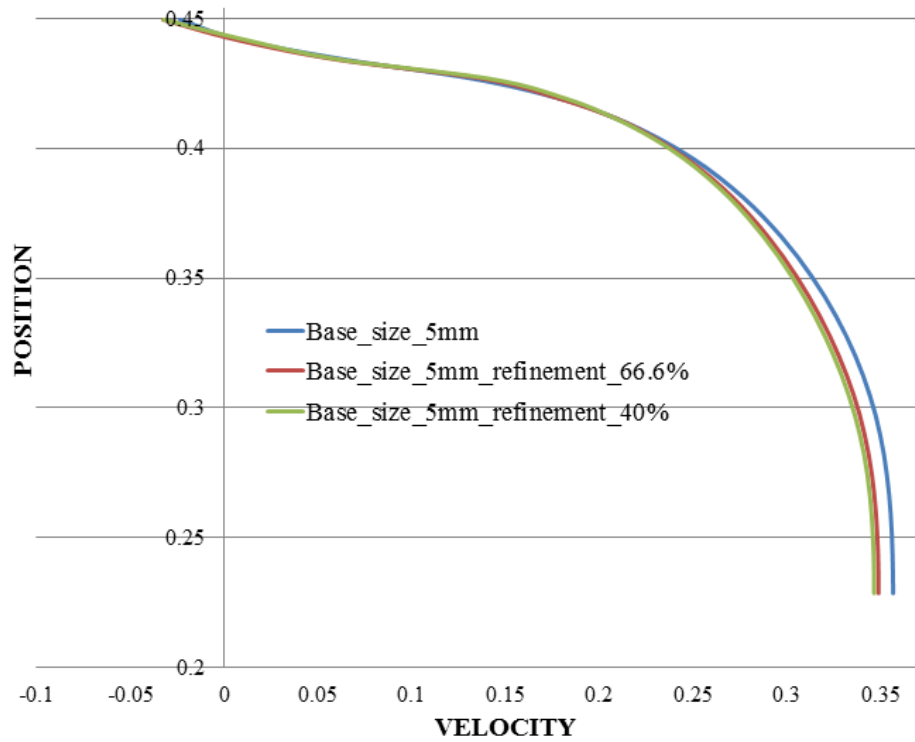
Figure 2.12: Velocity profiles of the different mesh cases with base size 5 mm plotted at a trough

In Figure 2.12, velocity profiles for the different mesh cases with base size 5 mm at a trough are plotted. The 5 mm base size with a 66.6% refinement in the trough appears to be the coarsest mesh that is mesh independent.
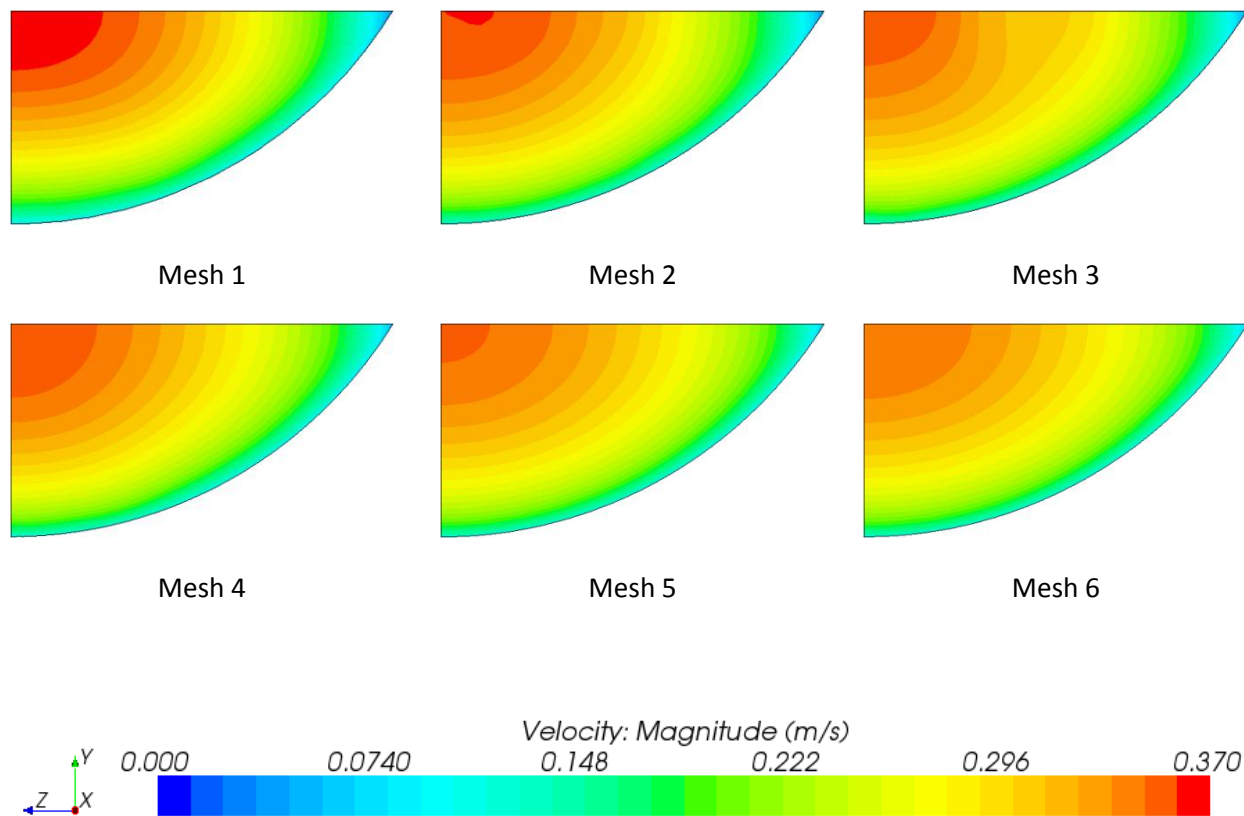
Figure 2.13: Velocity plots of the various mesh cases in the mesh refinement study

The above Figure 2.13 contains the velocity distribution scenes of all the various mesh cases used for the mesh refinement study plotted at a crest.

Mesh Refinement Conclusions: The mesh refinement studies have been conducted for various base sizes of the mesh for the symmetric reduced barrel section (considered from a trough to a trough) to choose the optimum base size of the mesh and also the refinement that needs to be done in the corrugated section. By analyzing the variation of the surface averaged velocity with respect to the length of the plane section at a trough and the velocity profiles plotted using line probes at a trough and a crest the optimum mesh can be selected. With all the CFD analysis done on a 36 inch diameter of the culvert with corrugation size 3 inches by 1, for a flow depth of 9 inches and a flow velocity of 0.71 feet/second for zero bed elevation of the culvert, in terms of mesh refinement studies, mesh 5 with a 5 mm base size and 67% refinement in the corrugation region, which yields a mesh with about 250,000 cells gives mesh independent simulation results with adequately fast run times.

2.3. Three Dimensional Model of Culvert Flume with Comparison to Experimental Results

The preliminary objective of this study was to develop a computational fluid dynamics (CFD) model to characterize the three-dimentional (3-D) two-phase (air and water) laboratory model associated with three different water depths, two different velocities and three bed elevations. The suitability of the CFD model for fish passage engineering analysis is assessed by comparison with experimental data obtained from TFHRC. In phase 1 of the study, a three-dimentional multi-phase CAD model, as shown in Figure 2.14, was created in Pro-ENGINEER. The CAD model consists of three parts along the flow direction (z axis): the intake, the barrel and the diffuser. Since the two-phase VOF model (water and air) is used for numerical simulation, initially an air layer was included on top of the water domain in the vertical direction (x axis). The culvert model considered in phase 1 of study is the symmetrical half of the culvert pipe having annular corrugations without bed elevation as shown in Figure 2.14.
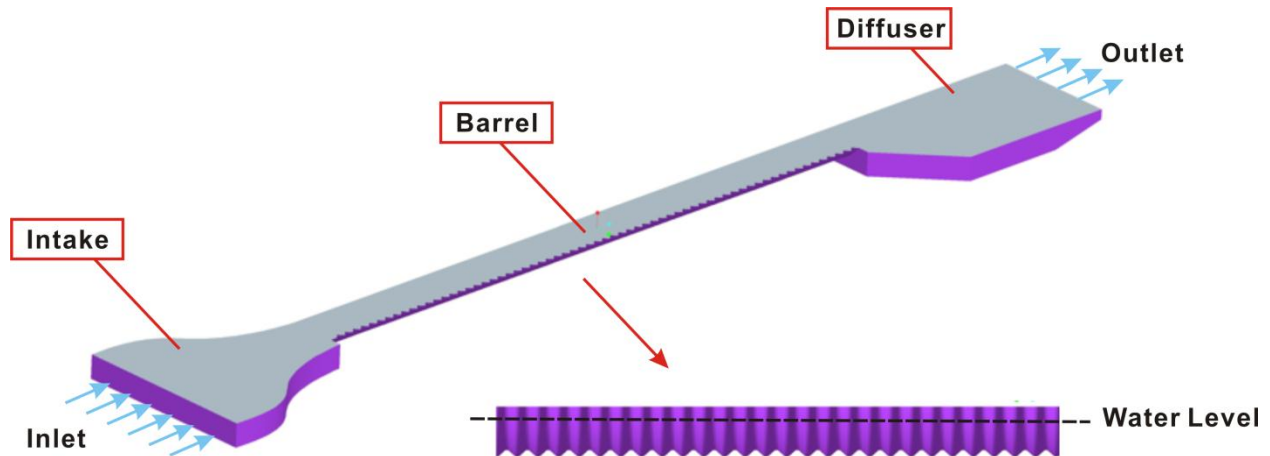

Figure 2.14: Three-dimensional CAD model for multi-phase simulations

The experiments in this study were conducted at the FHWA J.Sterling Jones Hydraulics Laboratory, located at the TFHRC. The experiments were conducted in a circulating flume. Figure 2.15 provides the details of the experimental flume dimensions in front and overlook views. The corrugations used are 3 inch by 1 inch annular. Three typical cross sections were monitored in the tests, which were located at the inlet of the barrel (section 1), the middle of the barrel (section 2) and the end of the barrel (section 3), respectively.
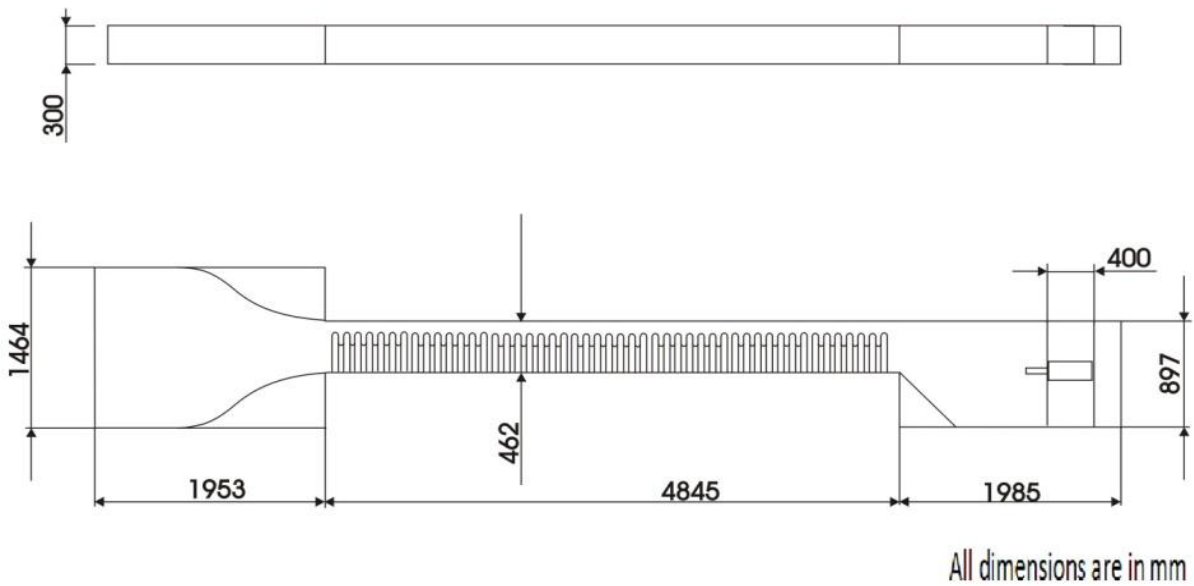
Figure 2.15: Dimensional details of the flume (front and top views)

The primary purpose of running CFD tests on a three dimensional model of the full TFHRC culvert test flume is to verify that the much smaller domain of a barrel section with cyclic boundary conditions can be used for parametric runs to determine zones for fish passage. A significant difference in the two models is that the small section using a cyclic boundary condition must be run as a single phase flow with a symmetric, free slip boundary condition at the water surface. This requires that the flow be deep enough for the corrugations to have negligible effect on the surface. Truncated CFD models with cyclic boundaries can be utilized as a time-effective tool in completing the large test matrix of the project.

2.3.1. Flow Conditions

All the test scenarios in the study involve three different water depths, two velocities, and three bed elevations. Additional design parameters include tilting angle of the flume, open angle of the flap gate, roughness parameters etc.. The flow conditions for the completed multi-phase CFD model tests are listed in Table 2.3.

Water Depth	3 inch	6 inch	9 inch
Bed elevation	0	0	0
Air depth(inch)	2.5	3	2.5
Mean velocity (m/s)	0.2164	0.2164	0.2164
Tilting angle of the flume (degree)	1	0.125	0.07
Tilting angle of the flap gate with respect to the horizontal (degree)	12.5	18	28

2.3.2. Results Using VOF Multiphase Model

Velocity distributions are plotted over a plane cut through a culvert barrel trough that is located in the middle of the culvert. For each water depth, the velocity distribution across the whole multi-phase cross-section is given on the left, and the plot on the right covers only the lower zone containing water. Also, the 0.5 VOF curves are plotted on top of the velocity contours, which indicate the corresponding water surface. The results for 3 inch, 6 inch, and 9 inch water depth are illustrated in Figure 2.16, Figure 2.17, and Figure 2.18 respectively.
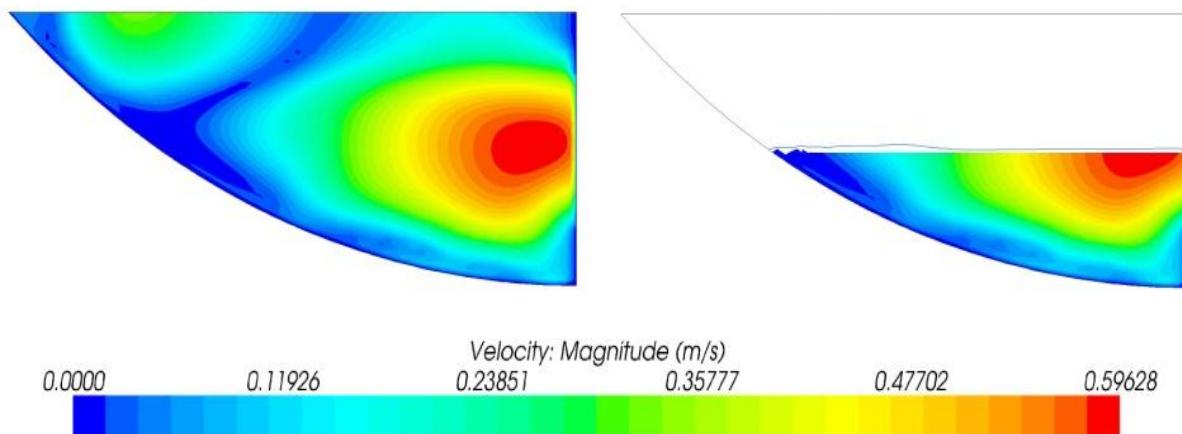

Figure 2.16: Velocity distribution across trough section of the multi-phase model for 3 inch water depth

Velocity: Magnitude (m/s)

| 0.0022006 | 0.079300 | 0.15640 | 0.23350 | 0.31060 | 0.38770 |
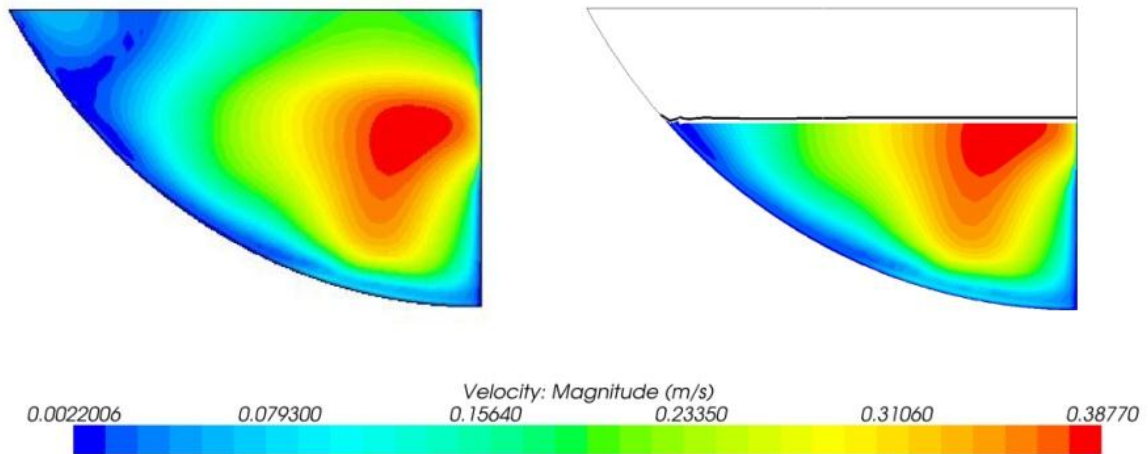
Figure 2.17: Velocity distribution across trough section of the multi-phase model for 6 inch water depth

Velocity: Magnitude (m/s)

| 0.0000 | 0.074056 | 0.14811 | 0.22217 | 0.29622 | 0.37028 |
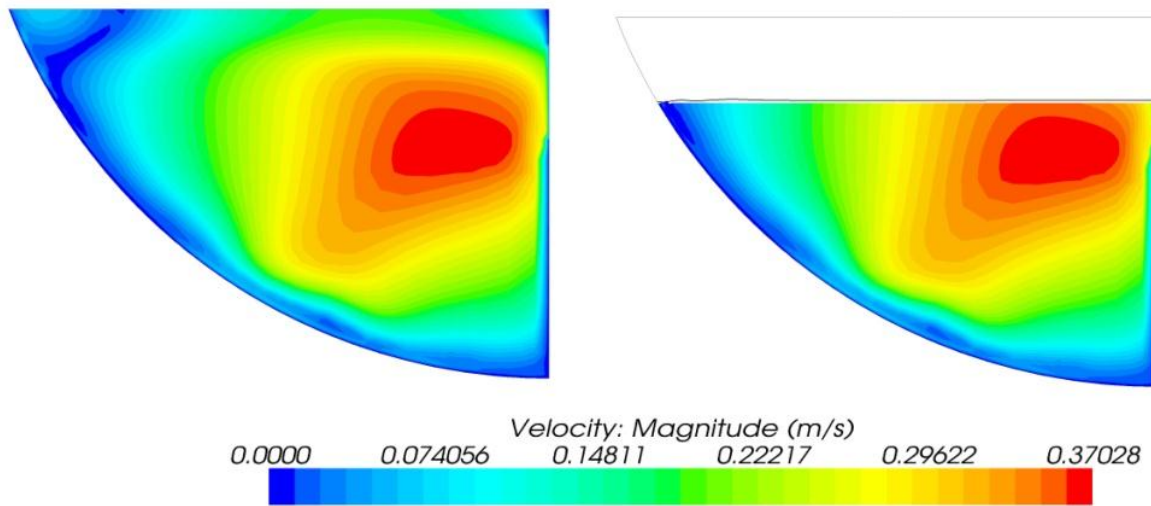
Figure 2.18: Velocity distribution across trough section of the multi-phase model for 9 inch water depth

2.3.3. Comparison with the Single Phase Model

In the multi-phase CFD model for the full-scale flume, if the longitudinal VOF changes indicate that the water level is nearly flat along the culvert, it is possible to set up a single phase model to simulate the flow. Figure 2.19 illustrates the comparison of the velocity distribution between the multi-phase model and full scale single phase model for 6 inch water depth. Note that the maximum velocity occurred in the single phase case is 0.42 m/s, which is larger than 0.38m/s in the multi-phase case.
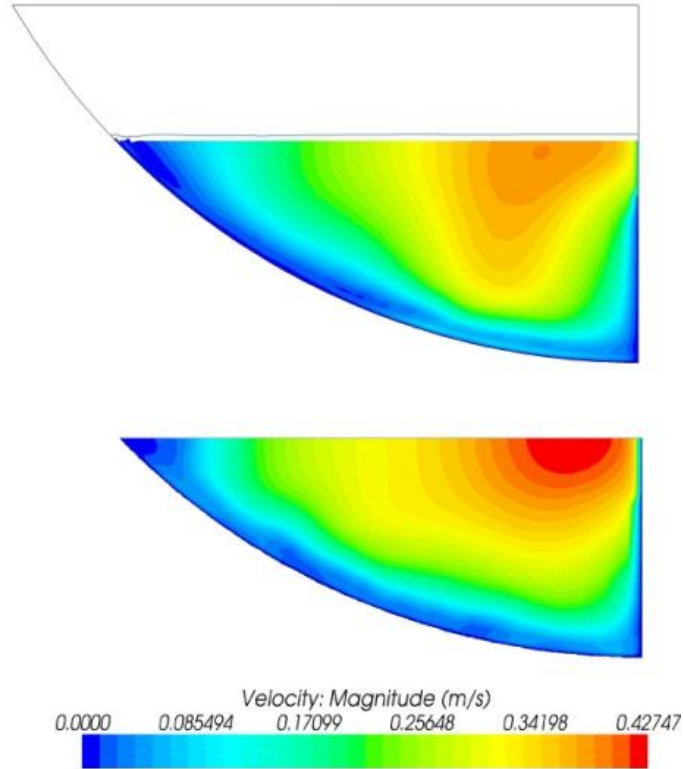
Figure 2.19: Multi-phase model vs. full flume single phase model illustrating velocity distribution across trough section for 6 inch water depth

2.3.4. Comparison with Laboratory Data

Particle Image Velocimetry (PIV) and Acoustic Doppler Velocimetry (ADV) are two methods used to capture the velocity data from laboratory experiments. Acoustic Doppler Velocimeters are capable of reporting accurate values of water velocity in three directions even in low flow conditions. The main objective of the PIV tests is to obtain a 3-dimensional high-resolution velocity distribution, which is convenient for visual comparisons with CFD results.

Comparisions of the CFD data with laboratory data for 6 inch and 9 inch water depths have been done. The agreement levels between multi-phase model results and experimental results for 6 inch water depth are depicted in Figure 2.20 and Figure 2.21. Since neither the PIV nor ADV can capture the data for the whole section, the corresponding data ranges are framed out in CFD results respectively.
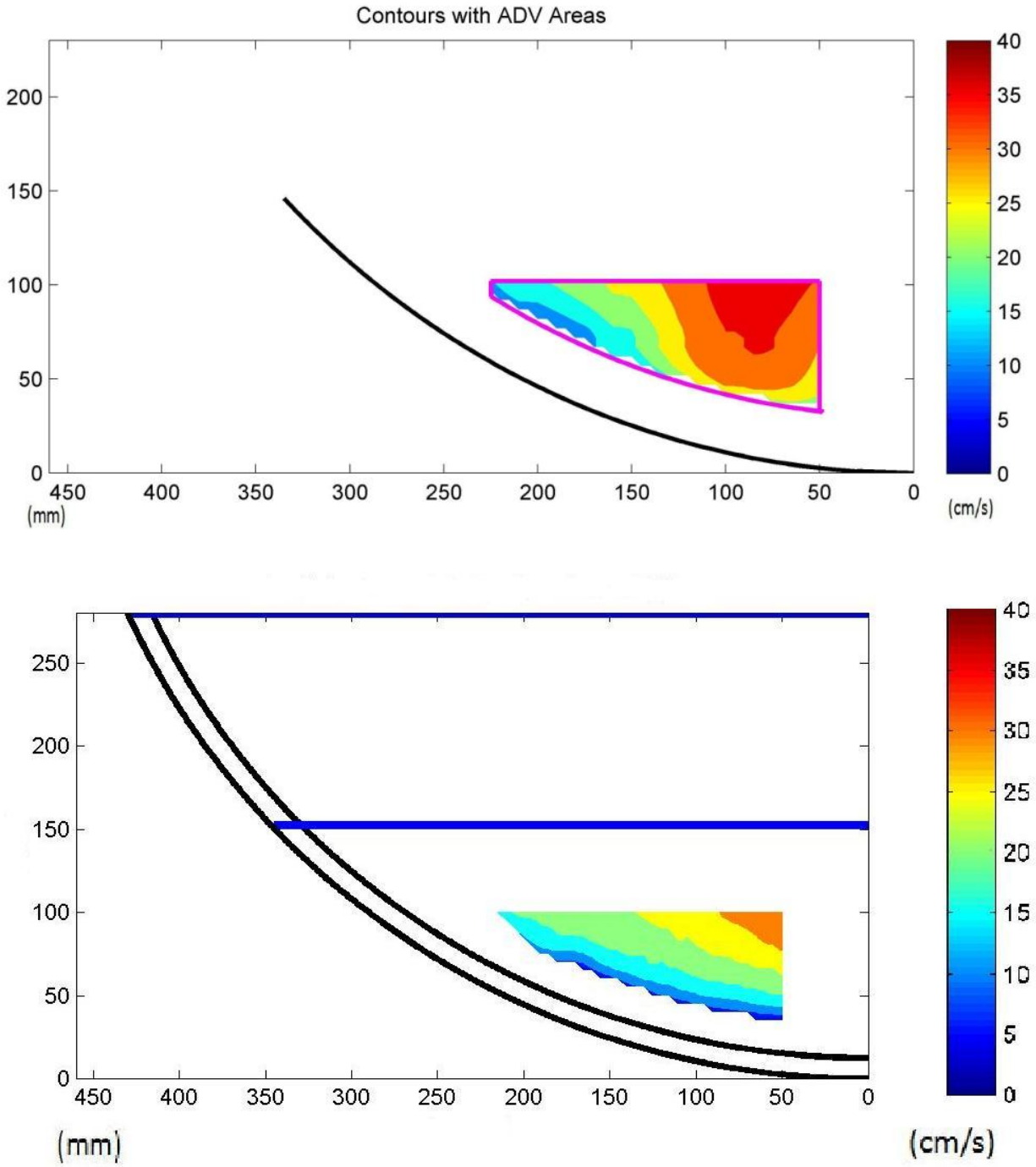
Figure 2.20: CFD velocity contour plot with ADV cut area (upper) vs. ADV velocity contour plot (lower) for 6 inch water depth on the trough section
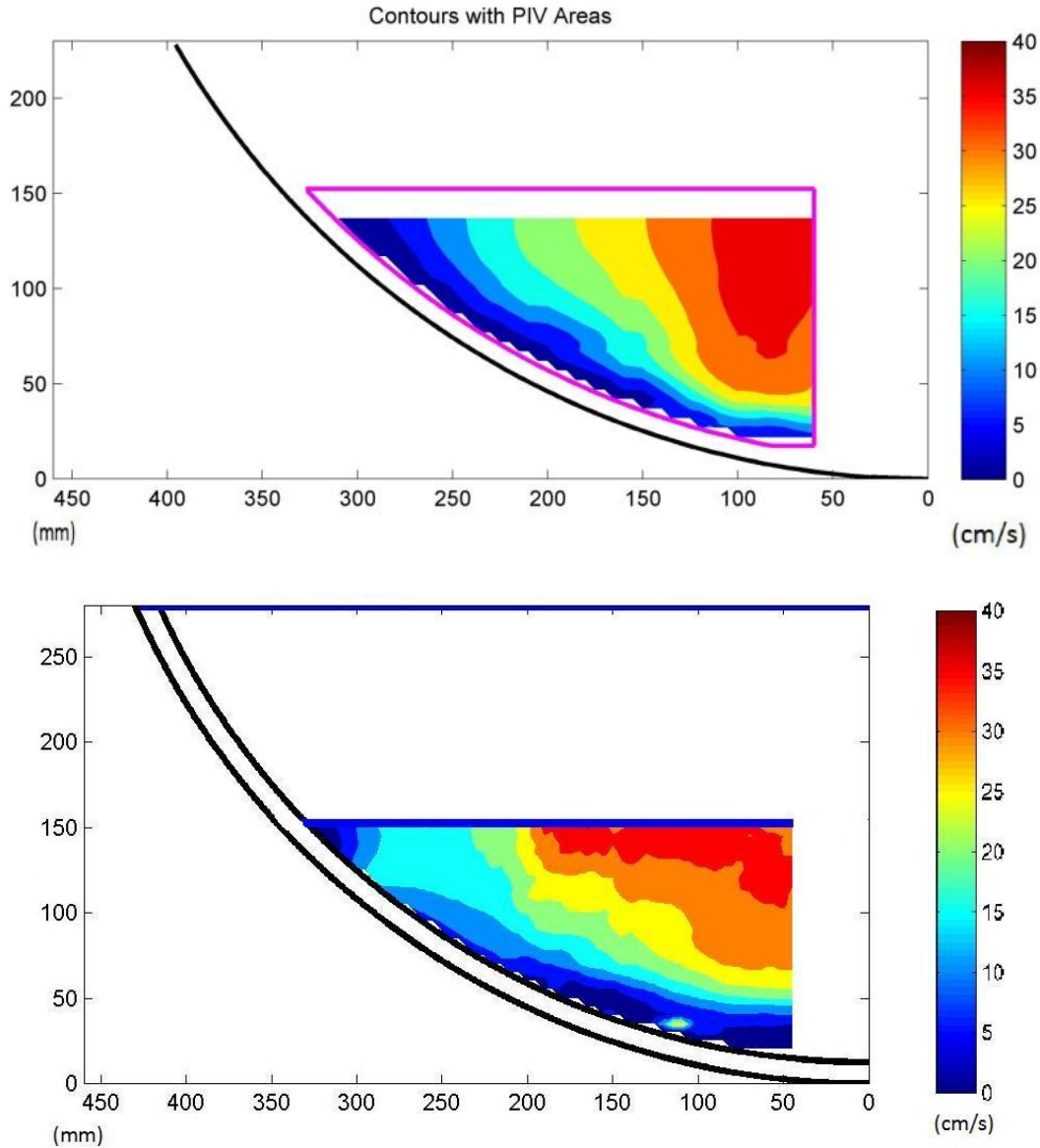
Figure 2.21: CFD velocity contour plot with PIV cut area (upper) vs. PIV velocity contour plot (lower) for 6 inch water depth on the trough section

The comparison between multi-phase CFD model results and ADV results for 9 inch water depth are shown in Figure 2.22, in which the comparable areas are much larger than those for 6 inch water depth. The comparison of multi-phase CFD results and PIV results for 9 inch water depth is still proceeding.
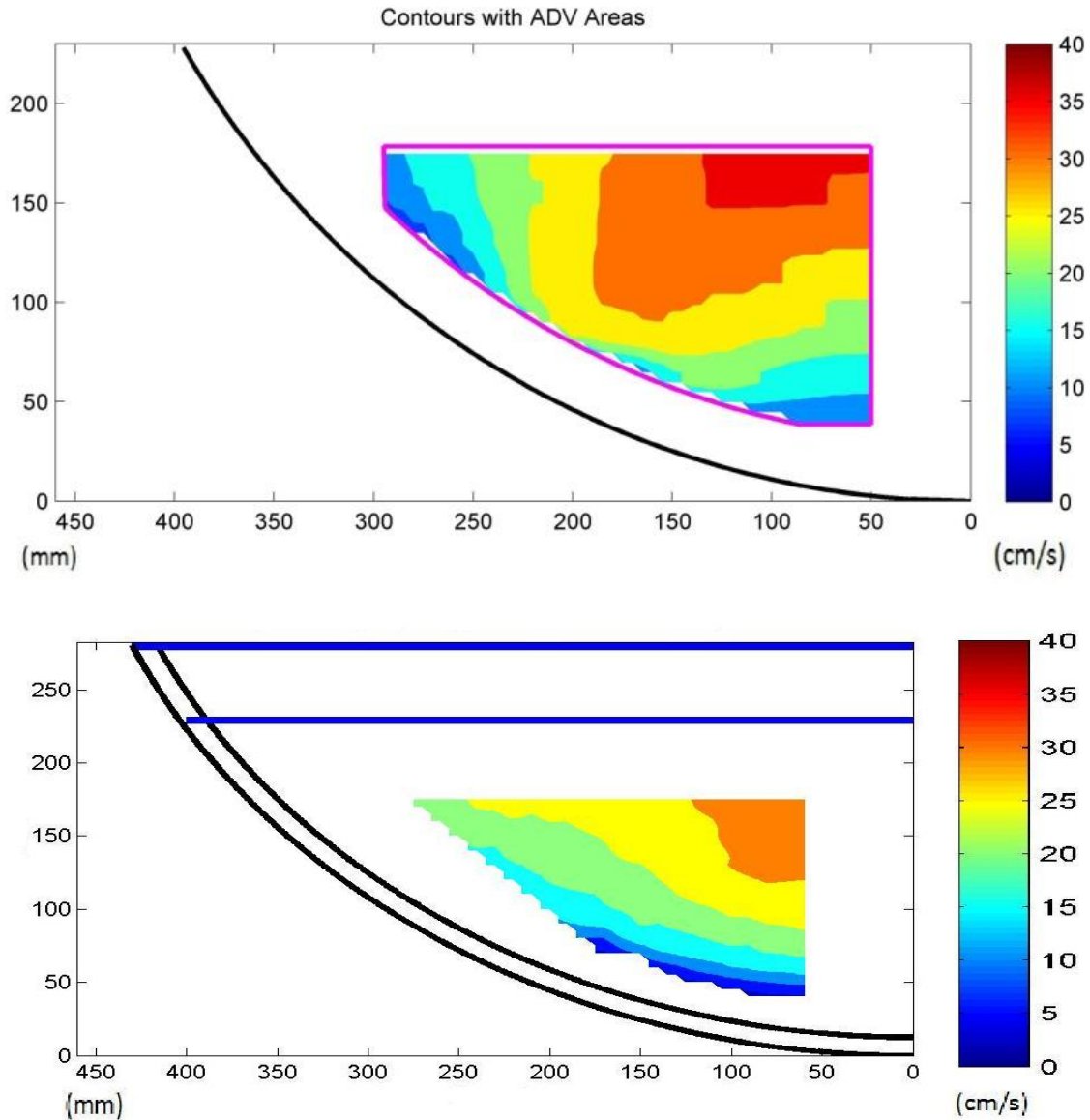
Figure 2.22: CFD velocity contour plot with ADV cut area (upper) vs. ADV velocity contour plot (lower) for 9 inch water depth on the trough section

The preliminary simulation results (for 0 bed elevation) reveal that the three-dimentional (3-D) two-phase (air and water) CFD models solved in STAR-CCM+ yield reasonably good agreement in the velocity distributions, compared with both the PIV and ADV data. The velocity distribution contours obtained from the CFD simulation are much closer to the PIV observation results. Furthermore, the PIV data capture range is larger than that of ADV because ADV can hardly get the data near the water surface and adjacent to the culvert boundary.

Note that the full flume single phase CFD model has better concurrence of velocity distribution with experimental measurements. Based on the discussion in Section 2.3.3, the single phase velocity

magnitude is larger than that of the multi-phase CFD model. Taking 90% of the magnitude of velocity obtained from the single phase CFD model, the visual agreement with the PIV results is presented in Figure 2.23.
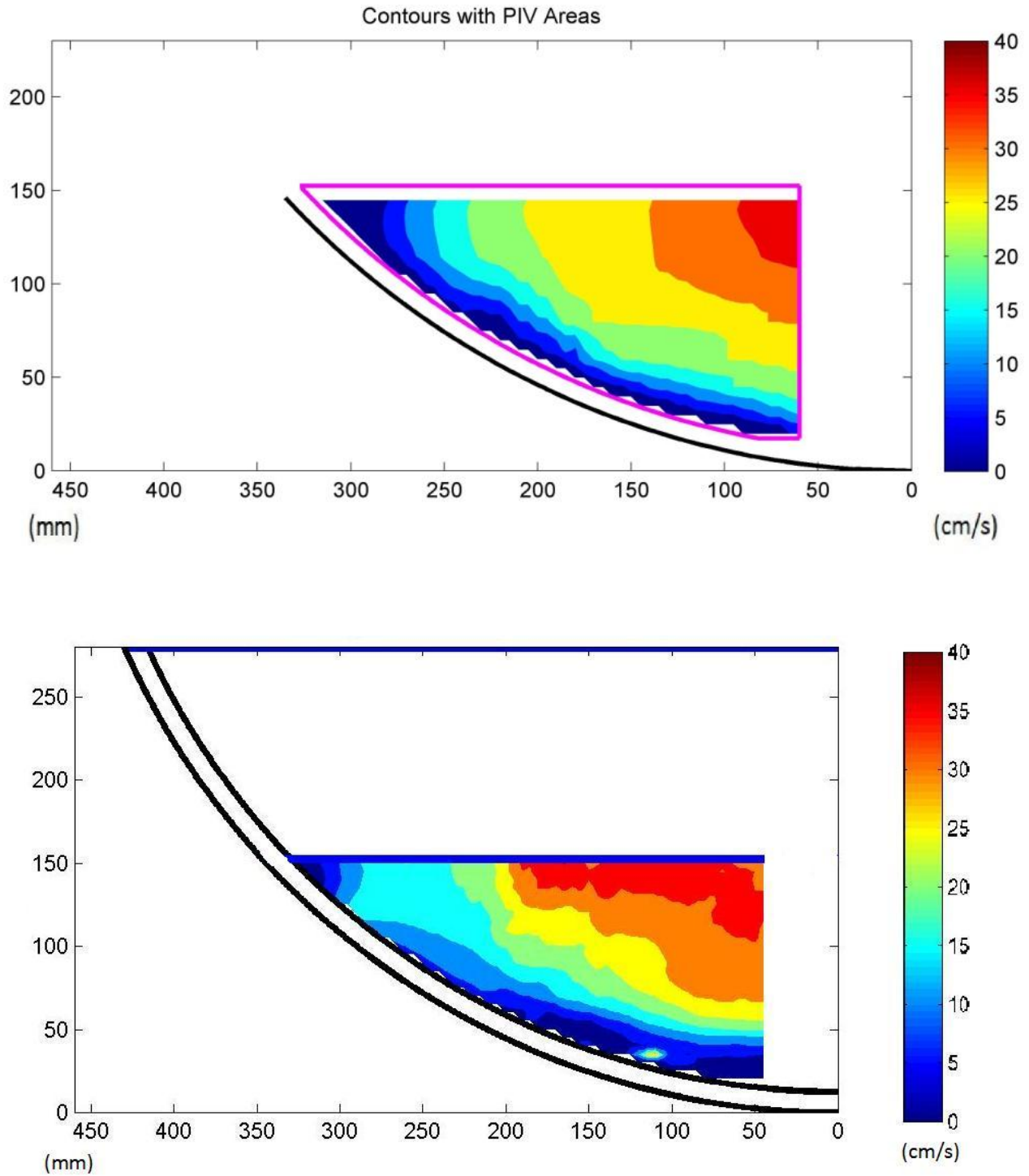

Figure 2.23: 90% single phase CFD velocity contour plot with PIV cut area from (upper) vs. PIV velocity contour plot (lower) for 6 inch water depth on the trough section

Conclusions for Comparisons with Experiment: The experimental work is not yet complete, and therefore this assessment is preliminary. The experimental PIV and ADV data show differences that are of the same order as the differences between either of the experimental approaches and the CFD results. All of these show significant variation of velocity over culvert cross sections with higher velocity near the center. Making engineering use of data obtained from CFD analysis on cross section variation of velocity will likely be an improvement over just using the mean velocity in design of culverts for fish passage. While there are differences in both of the experimental techniques and the multiphase and single phase CFD approaches to obtaining the cross section velocity distribution, the information is much closer to reality than an assumed uniform mean velocity. Culvert design for fish passage cannot come close to conditions that would exhaust fish attempting to swim through the culvert, and therefore the use of data that has some uncertainty but is much better than current practice can still yield a major improvement in design practice.

3.   References

1.   Matt Blank, Joel Cahoon, Tom McMahon, "Advanced studies of fish passage through culverts: 1-D and 3-D hydraulic modeling of velocity, fish expenditure and a new barrier assesment method," Department of Civil Engineering and Ecology, Montana State University, October, 2008 .

2.   Marian Muste, Hao-Che Ho, Daniel Mehl,"Insights into the origin & characteristic of the sedimentation process at multi barrel culverts in Iowa", Final Report, IHRB, TR-596, June, 2010.

3.   Liaqat A. Khan, Elizabeth W.Roy, and Mizan Rashid, "CFD modelling of Forebay hydrodyamics created by a floating juvenile fish collection facility at the upper bank river dam", Washington, 2008.

4.   Angela Gardner, "Fish Passage Through Road Culverts" MS Thesis, North Carolina State University, 2006.

5.   Vishnu Vardhan Reddy Pati, "CFD modeling and analysis of flow through culverts", MS Thesis, Northern Illinois University, 2010.

6.   Kornel Kerenyi, "Final Draft, Fish Passage in Large Culverts with Low Flow Proposed Tests" unpublished TFHRC experimental and CFD analysis of culvert flow for fish passage work plan, 2011.